ARTICLE

Characterization of hydrodynamics and volumetric power input in microtiter plates for the scale-up of downstream operations

Ignacio Montes-Serrano[1] | Peter Satzer[1] | Alois Jungbauer[1,2] | Astrid Dürauer[1,2]

[1]Austrian Centre of Industrial Biotechnology (acib GmbH), Vienna, Austria

[2]Department of Biotechnology, Institute of Bioprocess Science & Engineering, University of Natural Resources and Life Sciences, Vienna (BOKU), Vienna, Austria

Correspondence
Astrid Dürauer, Department of Biotechnology, Institute of Bioprocess Science & Engineering, University of Natural Resources and Life Sciences Vienna, Muthgasse 18, 1190 Vienna, Austria.
Email: astrid.duerauer@boku.ac.at

Funding information
H2020 Marie Sklodowska-Curie Actions, Grant/Award Number: 812909

Abstract

Parameter estimation for scale-up of downstream operations from microtiter plates (MTPs) is mostly done empirically because engineering correlations between microplates and stirred tank reactors (STRs) are not yet available. It is challenging to change the operation mode from shaken MTPs to large-scale STRs. For the scale-up of STRs, volumetric power input is well-established although it is unclear whether this parameter can be used to transfer the operations from MTPs. We determine the volumetric power input in MTPs via the temperature increase caused by the motion of the liquid. The hydrodynamics in MTPs are studied with computational fluid dynamics (CFD). Mixing is investigated in 96-, 24-, and 6-well MTPs to cover different geometries, filling volumes, shaking diameters, and shaking frequencies. All CFD simulations are validated by experimental results, which now allows prediction of the volumetric power input and hydrodynamics at various conditions in MTPs without the need for further experiments. We provide a map of the power input achievable in MTPs. Based on this map, from knowing about large-scale conditions, adequate microscale conditions can be adjusted for process development. This enables the direct scale-up of downstream unit operations from MTPs to STRs.

KEYWORDS
calorimetry, computational fluid dynamics, downstream processing, precipitation, scale up

1 | INTRODUCTION

Efficient scale-up of up- and downstream processing unit operations is upon the most crucial requirements for successful process development and transfer. Downstream operations dominate production costs in the production of biopharmaceuticals (Amanullah et al., 2003), with protein A chromatography being the most expensive component, as well as being the bottleneck of the manufacturing scheme (Somasundaram et al., 2018). Process engineers are

studying strategies to implement affordable unit operations while maintaining high product yields and purity. One operation of choice is typically precipitation, which is very efficient for the primary recovery of antibodies (Hammerschmidt et al., 2016; Satzer et al., 2020). However, the efficient scale-up of such unit operations is not straightforward. On the microscale, microtiter plates (MTPs) are increasingly used for high throughput screening (HTS) during process development in both upstream and downstream processing of biopharmaceuticals (Diederich et al., 2015; Effio & Hubbuch, 2015;

Feliciano et al., 2016; Hubbuch, 2012; Micheletti & Lye, 2006; Moreno-González et al., 2021; Schulze Wierling et al., 2005). They allow experimentation in a parallel fashion while reducing material consumption and enable high flexibility for the selection of operating conditions. However, the transfer from microscale to large-scale usually encounters challenges based on the change of the operation mode. In MTPs, mixing is mostly achieved by shaking, whereas in larger scale systems, it is usually achieved by stirring. This change in the mixing mechanism affects the hydrodynamics of the different scales. If we also consider continuous processing, there will even be other systems for mixing in place, for example, static mixers in tubes. Constant stirrer tip velocity, constant geometry, constant height/diameter, constant ratio of stirrer diameter to reactor diameter or volumetric power input are preferred engineering characteristics for scale up of STRs (Costes & Couderc, 1988). If it comes to the scale up from shaken small-scale systems such as shake flasks and MTPs to STRs those rules cannot be directly applied.

To overcome these limitations different approaches have been established for scale up of fermentation and cultivation processes as they were traditionally developed in shaken flasks. Büchs et al. (2000) established the dimensionless Phase number (Ph), the related Reynolds number (Re), and a minimum Froude number (Fr) of 0.4 as engineering characteristics for mixing in shaken flasks. Ph considers the ratio of the shaking diameter and the working volume to the inner diameter of the reactor and gives Ph>0.91 as the characteristic for the "in-phase" conditions which verifies homogenous flow and optimal mixing (Azizan et al., 2019). However, it does not seem to be the only criterion to ensure in-phase conditions, as Ducci and Weheliye (2014) considered that the in-phase conditions are dependent on the positioning of the velocity vector rather than the Ph number.

Another established parameter for scaling up fermentations and cell cultivations is by maintaining a constant oxygen transfer k_La, as shown previously (Doig et al., 2005; Wutz et al., 2018). Here, the critical shaking frequency, $n_{crit,}$ was established for 96-well MTPs which allows for careful adjustment of the conditions in those systems to optimize the oxygen transfer (Hermann et al., 2003). However, this parameter is not relevant for most downstream operations. Other approaches, such as conservation of mixing time in individual wells can also be used for the scale-up of mixing-dependent processes. Li et al. (2020) studied the mixing time in two different geometries, circular and square, of a 24-well MTP. They developed a strategy based on the natural frequency, enabling a comparison between their results and those obtained previously by Rodriguez et al. (2013) in large shaken reactors.

As constant volumetric power input as a strategy for the scale-up of STRs via the correlations of the Power number (Ne) and the Reynolds number (Re) is a common standard (Nienow, 2014), Büchs et al. (2000) have established modified Re and Ne values for shake flasks to allow a similar approach for those systems. Those modified numbers consider the inner diameter of the reactors as well as the working volume as impact factors on the mixing conditions (Büchs et al., 2000). They do not take the shaking diameter into account.

We propose a strategy to use power input as a scale-up parameter in combination with the evaluation of hydrodynamic conditions, extending this feature to shaken MTPs for the direct scale-up of unit operations involved in downstream operations.

We have recently determined the power input in MTPs with a clay/polymer flock system which correlates the floc destruction kinetics with the hydrodynamic stress (Dürauer et al., 2016). Here, we have also established a calorimetric method for the determination of the temperature increase caused by mixing in the individual wells as a reference method. Both methods determined the power input in the MTPs and were applied to three different geometries, 96-, 24-, and 6-well. We concluded that it is impossible to use volumetric power input only for direct scale-up from MTPs to STRs due to the changes in shear stress values between shaken MTPs and larger stirred vessels. To establish a strategy based on volumetric power input from MTPs to STRs, it would be necessary to determine the impact of different variables on the power input in more detail to determine the operation conditions of MTPs for process development. Further investigations of the fluid dynamics in MTPs would have been necessary.

We hypothesize that the shaking diameter has an impact on the power input and shear stress in shaken MTPs. We have therefore expanded our investigations on the mixing in MTPs, relating the inner diameter, the shaking frequency, the shaking diameter, and the filling volume to the power input determined by calorimetry. The use of computational fluid dynamics (CFD) allows for the characterization of the hydrodynamic phenomena in shaken MTPs (Salek et al., 2012; Wutz et al., 2018; Zhang et al., 2008). Previous investigations were conducted in the context of characterization of cell cultivation, but not in the context of downstream processing for the characterization of the motion of precipitates or other components required for separation processes. We therefore used CFD simulations to provide a better understanding of the hydrodynamics in the shaken MTPs. The aim was to obtain data for MTPs to generate an engineering correlation for a direct scale-up of downstream operations such as precipitation or flocculation from shaken MTPs to STRs.

2 | MATERIALS AND METHODS

2.1 | Calorimetric measurements

Three different MTPs, 96-, 24-, and 6-well plates, were used for the experimentation. All were clear, flat-bottomed polystyrene plates (ThermoFisher). The dimensions of the MTPs and the shaking conditions can be found in the Supporting Information Material. Two different orbital shakers were used: for the 3 mm diameter, a Thermomixer™ comfort (Eppendorf); for the 25 mm diameter, a Multitron (Infors HT).

The calorimetric determination of the temperature increase of the liquid needs adequate insulation to avoid fluctuations due to the

ambient temperature. The different MTPs were covered with a SealPlate® film (Sigma Aldrich) and placed inside a housing device manufactured by University College London (UCL). The housing consists of two parts: a body and a cover; MTPs are placed inside the body and the cover is placed on top. Two holes in the cover directly lead to two different wells from the MTPs, so the temperature of the well can be read directly with a temperature sensor. To insulate the system, the housing was covered with a 10 cm layer of Armaflex® (Armacell) and placed inside a Styrofoam™ box. The covered housing was placed on the shaker and left working for 12 h to reach entropic equilibrium (Dürauer et al., 2016). The temperature was tracked with SQUIRREL LOGGER 2010 (Grant Instruments) and was recorded every 10 s. PT100/4-L sensors (GREISINGER Electronic) were placed inside the individual wells. Temperature measurements were taken in three different positions: one outside the housing device to record the ambient temperature, the second placed inside an empty well to record the heat from the engine of the shaker, and the third inside a well filled with water. A schematic depiction of the device is shown in the Supporting Information Material. The recorded increase of temperature in the empty well was used to make corrections on the increase of temperature as calculated by Raval et al. (2007) (Equation 1):

$$mC_p \frac{dT}{dt} = UA(T_e - T) + P,$$ (1)

where m is the mass of the liquid in kg, C_p is the heat capacity of the liquid in J/(kg·K), U is the overall heat transfer in W/(m²·°C), A is the area of exposure in m², T is the liquid temperature in °C, T_e is the temperature of the engine in °C, and P is the heat generated from the motion in W. The power input can be obtained from the increase in temperature in the filled well with a correction from the value obtained in the empty well. This was calculated by determining the slope of the constant temperature increase of the liquid and corrected by obtaining the energy from the engine. The energy from the engine was calculated via the overall heat transfer coefficient ($U = 2.10\ W/(m^2°C)$), the area of exposure of the well and the temperature of the engine.

To determine the range of operation for the shaken wells, two limits were needed. The lower limit was defined by Hermann et al. as the critical shaking frequency (2003). This is the shaking frequency at which the mixture inside allows for a motion of the surface, enabling an adequate mixing (Equation 2).

$$n_{crit} = \sqrt{\frac{\sigma}{4\pi V_l \rho d_0}},$$ (2)

where n_{crit} is the critical shaking frequency in s⁻¹, σ is the surface tension in N/m², d_i is the inner diameter of the well in m, V_l is the volume of liquid in m³, and d_0 is the shaking diameter in m. The upper limit is determined by the highest shaking frequency at which the liquid is not spilled.

The constant Froude number has been used previously for scaling up mixed systems. We used it to compare the different investigated shaking conditions by the normalized Froude number as established by Tissot et al. (2010):

$$Fr = \frac{2\pi n \left(\frac{d_i + d_0}{2}\right)}{\sqrt{d_i * g}},$$ (3)

where n is the shaking frequency in s⁻¹ and g is the gravity in m/s². In this definition, both the shaking diameter (d_0) and the diameter of the well (d_i) are considered. Several differentiations have been developed for the study of the axial and radial Fr (Büchs et al., 2000; Weheliye et al., 2013).

Büchs et al. (2001) described a state in which shaken flasks exhibit "out-of-phase" conditions. These are met when the Froude number is below 0.4 and the Phase number, Ph, is below 1.26. The Ph was later adjusted to 0.91 (Azizan et al., 2019). It can be calculated via:

$$Ph = \frac{d_0}{d_i}\left(1 + 3_* \log_{10}\left(\frac{(2\pi n)\rho}{\mu} * \frac{d_i^2}{4} * \left(1 - \sqrt{1 - \frac{4}{\pi}\left(\frac{V_l^{\frac{1}{3}}}{d_i}\right)^2}\right)^2\right)\right).$$ (4)

According to the established working conditions, none of our experiments in the MTPs would have a value lower than 0.4 for the Froude number, hence, the determination of whether they are in-phase according to this criterion is dependent on whether they reach a value of 0.91 for Ph.

2.2 | CFD

The CFD simulations were performed using Star-CCM+ V.12.02.011 (Siemens). All the simulations were performed for individual wells of MTPs using the trimmed mesh technique. To implement a laminar behavior the geometry was subdivided into 2.5×10^5 cubic elements, as shown by Wutz et al. (2018), enabling adequate modeling and reproduction of the experimental results. Simulations with coarser meshes were performed to try to reduce the computational time, but they did not fully model the motion of the wells. The chosen model is the volume of fluid (VOF) model, which allows for the adequate capture of the free surface in these simulations. This method assumes that the fluid phase domain is simply connected without interaction between them (Salek et al., 2012). The conservation equations are obtained from the Navier–Stokes model:

$$\frac{\partial \rho}{\partial t} + \nabla \cdot (\rho \vec{v}) = 0,$$ (5)

$$\frac{\partial (\rho \vec{v})}{\partial t} + \nabla \cdot (\rho \vec{v}\,\vec{v}) = -\nabla p + \nabla(\mu \nabla \vec{v}) + \rho \vec{g} + \vec{F_\sigma},$$ (6)

where p, t, v, and F_σ are the pressure in Pa, time in s, velocity in m/s, and surface tension force in N/m^2, respectively. For the interface, the resolution is performed with a modification of Equation (6), which implements the volume fraction of the phases:

$$\frac{1}{\rho_i}\left[\frac{\partial(\alpha_i\rho)}{\partial t} + \nabla\cdot(\alpha_i\rho_i\vec{v_i})\right] = 0, \tag{7}$$

where α is the volume fraction of the phase and i refers to the studied phase. The sum of both fractions needs to fulfill the condition:

$$\Sigma_{i=1}^{n=2}\alpha_i = 1. \tag{8}$$

This allows for the determination of the fraction for each of the components by only knowing some of them. With such conditions, the density and viscosity of the mixture at the interface can be calculated as:

$$\rho = \alpha_{L*}\rho_L + (1 - \alpha_L)_*\rho_G, \tag{9}$$

$$\mu = \alpha_{L*}\mu_L + (1 - \alpha_L)_*\mu_G. \tag{10}$$

The well undergoes a circular motion as it circulates an established orbit implemented by the platform of the shaker. The reference frame for the motion is described with a Cartesian coordinate frame placed at the distance of the orbital diameter from the center of the well and a cylindrical coordinate frame placed in the center of the well. The z-axis is reserved for the vertical axis, with the gravitational force occurring in its negative direction. The movement is described as:

$$v = \begin{bmatrix} v_x \\ v_y \\ v_z \end{bmatrix} = \begin{bmatrix} d_0\Omega\cos(\Omega t) \\ d_0\Omega\sin(\Omega t) \\ 0 \end{bmatrix}, \tag{11}$$

where Ω is the angular velocity in rad/s. The motion of the mesh is inserted with the use of the moving mesh instead of the moving reference frame, as it allows for better convergence and reduces the computational time for the solution (Wutz et al., 2018). The volumetric power input is calculated with the viscous energy dissipation (Zhang et al., 2008). The energy dissipation is calculated with the gradients of velocities within the system:

$$\phi_V = 2\left[\left(\frac{\partial v_x}{\partial x}\right)^2 + \left(\frac{\partial v_y}{\partial y}\right)^2 + \left(\frac{\partial v_z}{\partial z}\right)^2\right] + \left[\frac{\partial v_x}{\partial y} + \frac{\partial v_y}{\partial x}\right]^2$$
$$+ \left[\frac{\partial v_z}{\partial x} + \frac{\partial v_x}{\partial z}\right]^2 + \left[\frac{\partial v_z}{\partial y} + \frac{\partial v_y}{\partial z}\right]^2, \tag{12}$$

with ϕ_V as the energy dissipation of the system in s^{-2}. The volumetric power input can be obtained by applying such terms as:

$$\frac{P}{V} = \frac{\int_V \mu\phi_v dV}{V}. \tag{13}$$

The calculation of the volumetric power input in the simulations is performed by implementing a threshold with the volume fraction of the water and correcting Equation (13) with the addition of the phase fraction inside the integration Wutz et al. (2018):

$$\frac{P}{V} = \frac{\int_V \alpha_L\mu\phi_v dV}{V}. \tag{14}$$

CFD always requires validation by experimental data. This validation is done by comparing the values of the volumetric power input obtained from calorimetric experiments to those determined by the CFD simulations.

The definition of energy dissipation was stated above in Equation (12) as the addition of the different gradients of velocities in the motion of the fluid. One term linked to this parameter is the shear rate and shear stress. The definition of the shear rate is:

$$\gamma = \left(2\left[\left(\frac{\partial v_x}{\partial x}\right)^2 + \left(\frac{\partial v_y}{\partial y}\right)^2 + \left(\frac{\partial v_z}{\partial z}\right)^2\right] + \left[\frac{\partial v_x}{\partial y} + \frac{\partial v_y}{\partial x}\right]^2 \right.$$
$$\left. + \left[\frac{\partial v_z}{\partial x} + \frac{\partial v_x}{\partial z}\right]^2 + \left[\frac{\partial v_z}{\partial y} + \frac{\partial v_y}{\partial z}\right]^2\right)^{1/2}, \tag{15}$$

with γ being the shear rate in s^{-1}. This parameter is used for the study of the velocity gradient and the distribution of the energy dissipation.

2.3 | Volumetric power input in STRs

In this approach, the power required on the large scale is used to calculate Ne, which then makes it possible to obtain the corresponding Reynolds number, Re, from the tabulated curves (Amanullah et al., 2003). With these values, it is possible to determine conditions at different scales (Nienow, 2014).

$$Re = \frac{n\ D_i^2\rho}{\mu}, \tag{16}$$

$$N_e = \frac{P}{\rho n^3 D_i^5}, \tag{17}$$

where n is the stirring frequency in s^{-1}, D_i is the diameter of the impeller in m, ρ is the density of the fluid in kg/m^3, μ is the dynamic viscosity in Pa·s, and P is the power in W.

3 | RESULTS AND DISCUSSION

The volumetric power input was determined by calorimetric measurements and related to the shaking frequency, the inner diameter of the well, the shaking diameter, and filling volume. For a better understanding of the results, the same motion was simulated using CFD to obtain the hydrodynamics.
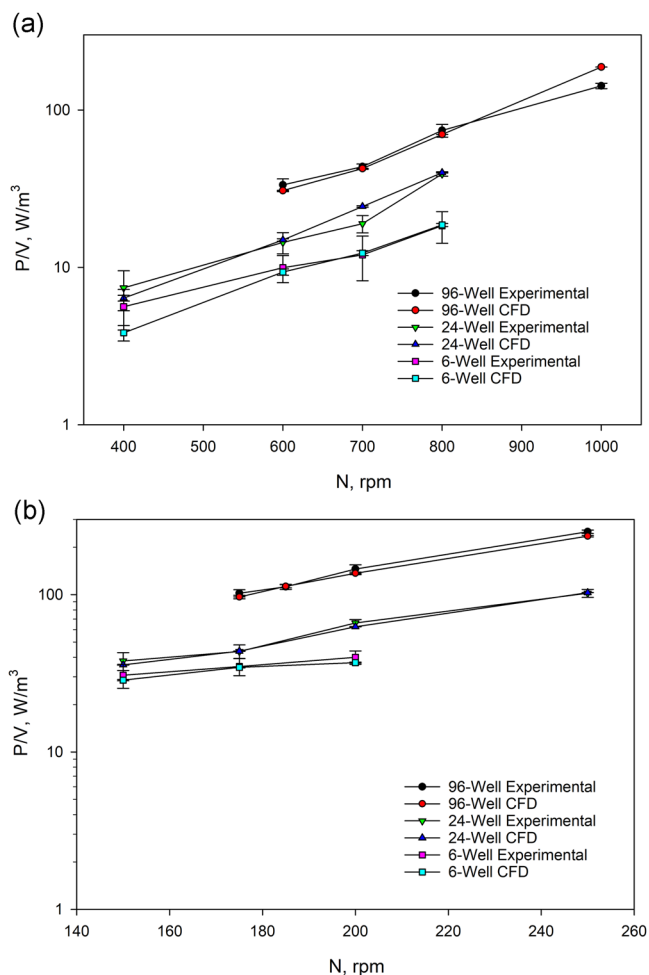
3.1 | Calorimetric measurements

For the calorimetric measurements, determined with the temperature increase in shaken MTPs upon mixing, one important consideration is the possible evaporation of water over time and the impact of the ambient temperature in the well, as a measure for the quality of insulation. The latter measurements, the ambient temperature, and the temperature inside the wells were measured without any motion for 12 h, which was the typical duration of one experiment. The results showed deviation in the ambient temperature over time which did not translate to the temperature measured inside the well. Therefore, it is assumed that the heat transfer from the ambient temperature to the water can be neglected. Evaporation was studied using a method as described by Sieben et al. (2016), which uses a solution of pH indicator and implies the measurement of the absorbance to determine the amount of liquid that has been evaporated. Two more methods, visual and weight, were used to validate the results from the absorbance measurements. This was performed by observing the initial and final height, as well as the weight of the MTPs before and after the process. Overall, the maximum loss of

water over time was 2%, thus it was assumed that the impact of evaporation can be ignored.

As already reported (Dürauer et al., 2016), the increase of temperature caused by the mixing in the MTPs followed a constant increase until it reached the equilibrium value of entropy, leading to constant values of temperature over time (Figure 1). The volumetric power input was calculated from the slope of the linear increase, which displayed a constant value of the energy dissipation (Ducci & Weheliye, 2014). The working conditions for the different wells can be found in the Supporting Information Material. Independently of the size of the individual well, a higher shaking frequency led to a faster temperature increase and higher equilibrium temperatures (Figure 1a–c). Higher shaking frequencies led to higher velocities of the liquid. These eventually led to a greater gradient of velocities, thus, a more significant amount of energy dissipation, causing a higher temperature increase. For the 96-well microplate, the volumetric power input increased from 31 to 190 W/m^3 when the shaking frequency was increased from 600 to 1000 rpm on an orbital shaker of 3 mm in diameter (Figure 2a).
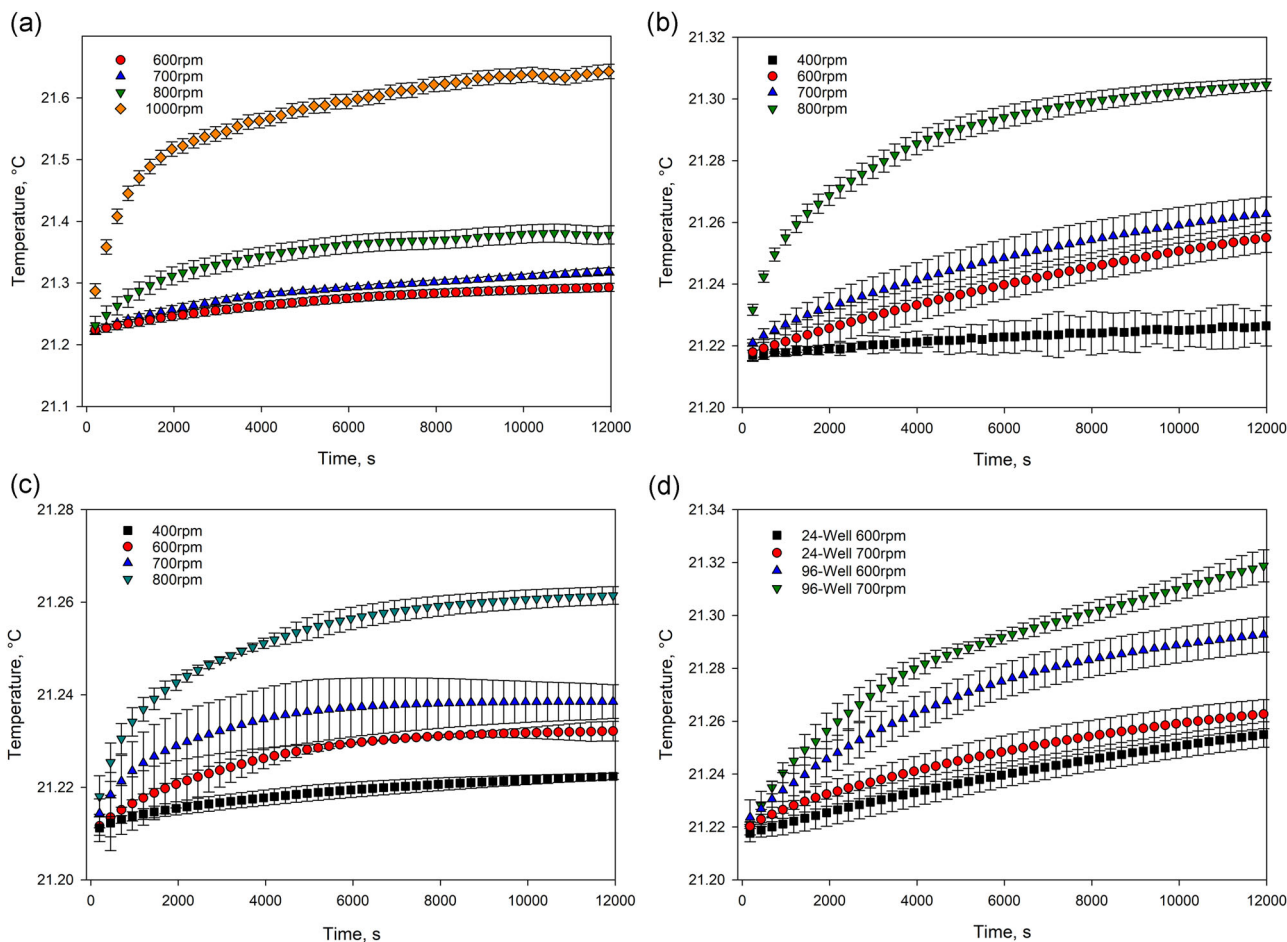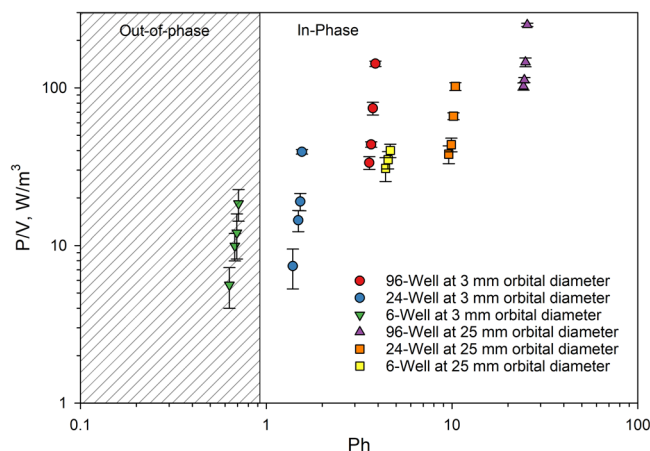

FIGURE 1 Temperature increase for individual wells of three microplates on a 3 mm shaking diameter and increasing shaking frequencies: 96-well (a), 24-well (b), 6-well (c) microtiter plates and comparison of the temperature increase for individual the wells of 96- and 24-well microplates at shaking frequencies of 600 and 700 rpm (d)

(a)

(b)

FIGURE 2 Comparison of volumetric power input obtained by calorimetric measurements and CFD simulations for individual wells of 96-, 24-, and 6-well microplates on increasing shaking frequencies for two different shaking diameters: 3 mm (a) and 25 mm (b). CFD, computational fluid dynamics

FIGURE 3 Volumetric power input versus Phase number for three different wells, 96-, 24-, and 6-well under two different shaking diameters, 3 and 25 mm, with the establishing of a frontier between the out-of-phase and in-phase conditions

Additionally, a significant impact of the geometry of the microplate on the volumetric power input was found. The increase of temperature was more prominent in the 96-well plate than the 24-well plate, at 600 and 700 rpm on the 3 mm orbital shaker (Figure 1d). The volumetric power input determined on this shaker at 600 rpm was 31, 15, and 9 W/m^3 for the 96-, 24-, and 6-well plates, respectively (Figure 2a). As the inner diameter increased from 96- to 6-well plates, the volumetric power input decreased. One reason might be higher friction in the 96-well plate compared with the 24-well plate, since the surface-to-volume ratio is higher in the 96-well plate. For 96-well plates, this ratio was calculated to be 755 m^{-1}, while it was 506 m^{-1} in a 24-well plate. The contact with the walls creates a gradient of velocities between the wall and the neighboring regions due to friction. This gives a possible explanation for why the increase of temperature in the 96-well plate was higher than in the 24-well plate (Dürauer et al., 2016).

Figure 3 shows different values of volumetric power input for different Phase numbers Ph in different wells on shakers with

different shaking diameters. Büchs et al. (2001) stated a decay in the power input when they were in out-of-phase conditions. Figure 3 displays the results for the 96- and the 24-well plates in the in-phase area. The lack of in-phase conditions might also be a reason for the low values of power input. However, it cannot be the only reason because some working operations for the 24-well plate have the same volumetric power input and are in-phase.

Previous results regarding the impact of shaking diameter on volumetric power input have been contradictory. While Büchs et al. (2000) did not find a correlation between the power input and the shaking diameter, our previous investigations indicated an increase of power input with an increase of the shaking diameter based on the clay floc destruction kinetics (Dürauer et al., 2016). These were also aligned with the findings of Zhang et al. (2008). Therefore, we extended our investigation to measurements of the temperature increase in MTPs on a 25 mm orbital diameter. The experiments were compared according to their similar Froude number. In this case, the selected conditions for the 96-well plates were 600 rpm on the 3 mm shaker (Fr = 1.20) and 175 rpm on a 25 mm orbital diameter shaker (Fr = 1.15). These were the conditions leading to the closest Froude numbers possible in these two systems using the Froude number equation (Equation 3). The observed trends showed a higher increase of temperature for the higher shaking diameter (Figure 4), increasing the volumetric power input to 96 W/m^3 for a shaking diameter of 25 mm compared with 31 W/m^3 on the 3 mm shaker. The results obtained for all the MTPs on the 25 mm shaker are shown in Figure 2b. These results show that the conservation of the ratio between flow velocity and the propagation of the waves at different conditions, as indicated by the conservation of the Froude number (Equation 3), might not be enough to maintain the same volumetric power input when shaking on different shaking diameters. Rather, it might be the difference of linear velocity in the wells that leads to a higher gradient on the walls for larger shaking diameters, granting the more pronounced increase of temperature and, thus, a more
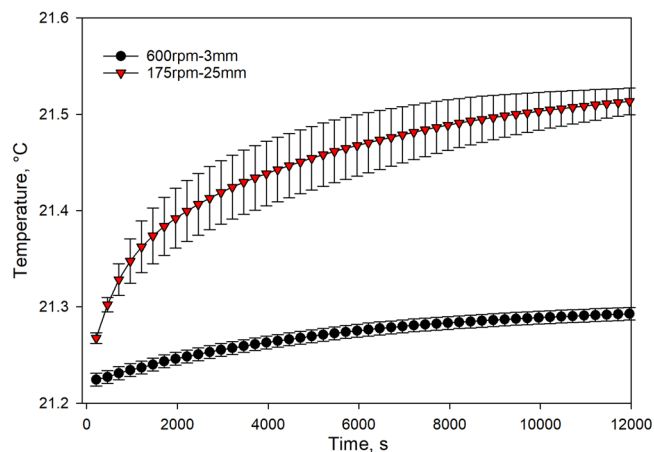
FIGURE 4 Temperature increase in an individual well of 96-well microtiter plate on a 3 mm shaking diameter and shaking frequency of 600 rpm and a 25 mm shaking diameter and a shaking frequency of 175 rpm. Conditions were chosen according to the similar Froude number

significant volumetric power input for the 25 mm orbital diameter. The limitations of the working operations with the different wells, however, could not guarantee reaching an optimum, thus missing possible opportunities for the design of purification steps.

3.2 | CFD

In addition to the results obtained by the calorimetric measurements, the hydrodynamics in the shaken MTPs must be understood to allow an engineered scale-up to large and/or continuous mixed systems. Our previous results obtained by the clay floc destruction method gave the first insight into the shear stress in the MTPs. The use of CFD simulations allows us to understand the hydrodynamics in different types of systems and can be utilized to study the flow patterns of the MTPs. These can give useful insights into how the system behaves and how it can be optimized.

3.2.1 | Validation of simulations

CFD simulations always require experimental validation to demonstrate adequate modeling. Therefore, the volumetric power input results obtained from the CFD simulations were compared with those calculated by the calorimetric measurements (Figure 2). All the performed simulations were carried out for laminar flow conditions. The observed results from CFD are in good agreement with the results obtained from the calorimetry, with only minor deviations occurring in the extreme conditions of the shaking frequencies —below 400 rpm and higher than 800 rpm—on the 3 mm shaker (Figure 2a). Although the system is always in laminar flow, CFD usually has limitations for certain conditions of the motion, especially when treating larger scales (de Lamotte et al., 2018). Good

accordance between the CFD simulation and experimental data is essential to perform simulations at conditions outside the actual working space of the MTPs and evaluate their impact without the need for further experiments. The inner diameter of the wells, for example, cannot be adjusted freely in an experimental setup, but CFD can simulate their theoretical impact on the power input. With this validation, the simulations are adequate to study the hydrodynamic effects produced within the wells. One of the studied features refers to how the increase of temperature is related to the motion of the fluid, as stated above. The results obtained from shaken MTPs at 25 mm orbital shakers are in the range of those determined in shaken flasks, which are usually between 100 and 1000 W/m^3 (Peter et al., 2006). However, our results do not reach the higher values due to the operating limits as mentioned above, leading to a limitation of the MTPs to cover operations that require volumetric power input higher than 250 W/m^3.

3.2.2 | Shear rate and linkage with calorimetry

Figure 5 displays the heat map of shear rate for an individual well of a 96- or a 24-well MTP shaking at 600 rpm (A, B) or 800 rpm (C, D) on a 3 mm orbital shaker. These conditions were selected because of the significant difference in volumetric power input between them, allowing for a better analysis. There is a direct relation between shear rate and energy dissipation, as shown by comparing Equations (12) and (15), so the increase of shear rate means a direct increase of energy dissipation. The impact of the inner diameter of the well on the energy dissipation can be observed from the comparison of Figure 5a with 5b and 5c with 5d. The heat map shows differences between how the gradient is distributed inside a well of a 96- and a 24-well plate. As already determined by the temperature measurements, values of energy dissipation rise with the increase of shaking frequency. The significant impact of the shaking diameter on the hydrodynamics and energy dissipation in the well is shown by the CFD simulations (comparing Figure 5a with 5e). A more in-depth observation was performed by obtaining the heat map and velocity contour of a transversal cut through the wells made at a fifth of the height of the liquid when the system did not undergo any motion (see Figures in the Supporting Information Material). The obtained results display areas with larger values of shear rate for the 96-well plates than the 24-well plates, leading to the larger values of volumetric power input. These results, however, show the velocity contours of the 96-well plate pointing in different directions, even creating certain toroidal vortexes for the 25 mm orbital diameter. The results from Figure 3 show that, according to the Phase number, these systems should be in-phase. Nevertheless, the discussion by Ducci and Weheliye (2014) seems to point toward out-of-phase conditions when looking at the motion of the velocity contour. Following such criteria, the effect seems to be the opposite to the one shown by Büchs et al. (2000). The value of the volumetric power input would be more significant on systems that are out-of-phase than those that are in-phase.
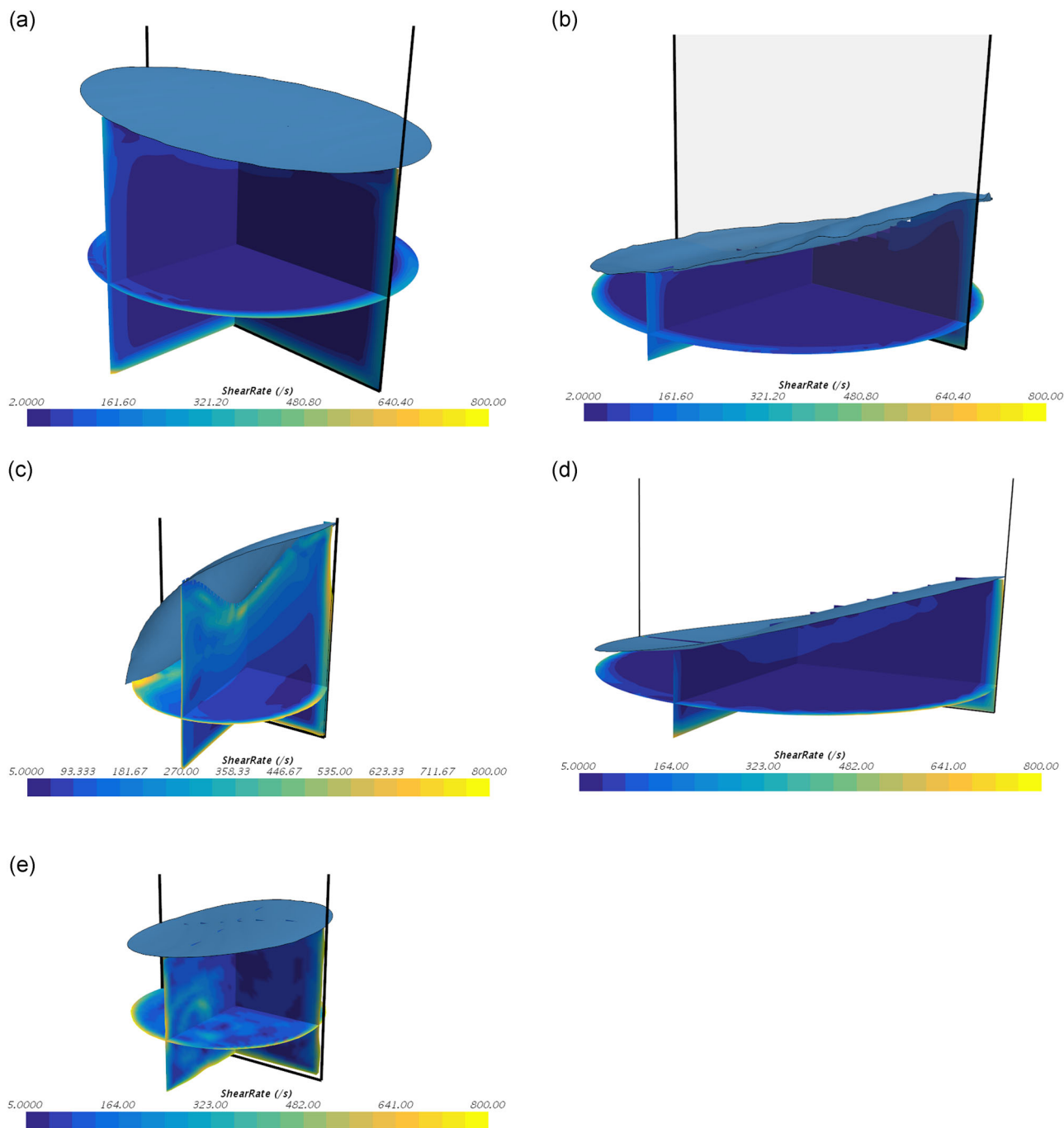
FIGURE 5 Heat map of the strain rate on the liquid phase for individual wells of 96- and 24-well microplates under different shaking conditions: 96-well (a) and 24-well (b) shaken at 600 rpm; 96-well (c) and 24-well (d) shaken at 800 rpm; both on a 3 mm orbital shaker. 96-well shaken at 175 rpm on a 25 mm orbital shaker (e)

For comparison between the wells, the calculated shear rate was obtained as the integral value (see Supporting Information Material). The shear rate increased with increasing shaking frequency, inner diameter, and volume of the well. The lower shear stress in the 96-well plates compared with the 6-well plates has already been shown via the clay floc destruction method used in our previous research (Dürauer et al., 2016) as well as by Wutz et al. (2018). Recent results also confirm the impact of the shaking diameter on the shear rate, which could be limiting for choosing the operation conditions for the development of different downstream processes such as the conditions for the precipitation of antibodies, since it can compromise the particle size distribution of the precipitates (Satzer et al., 2020). Thus, for those unit operations, the decision of the system cannot only rely on the conservation of volumetric power input.
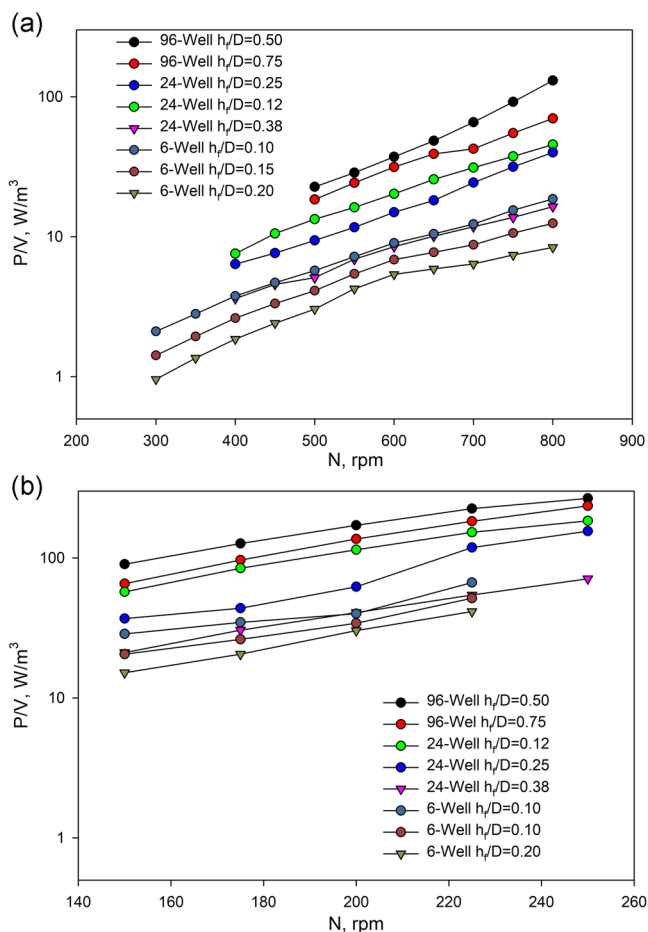
3.2.3 | Study of different filling volumes

The validation of the CFD modeling allows us to study additional conditions which might be of interest to understand the mixing mechanism and to suggest optimized working conditions. The working volume in MTPs is usually recommended by the manufacturer as a suitable range of volumes. The change of working volume influences the volumetric power input, as shown by Büchs et al. (2001) for shaken flasks. Therefore, the effect of different filling volumes on the hydrodynamics in MTPs was investigated by CFD. The filling volumes were selected according to ratios between the height of the fluid to the diameter of the wells. A list of the studied ratios and filling volumes is given in the Supporting Information Material. The 96-, 24-, and 6-well MTPs had different height-of-fluid-to-diameter ratios as the geometry did not allow us to adjust to the same ratios. With an increasing filling volume, the volumetric power input decreased for the same mixing conditions (Figure 6), explained by the decrease of the surface-to-volume ratio discussed above. The ratio in a 96-well plate is 850 and 755 m^{-1}, respectively, for $h_f/D = 0.5$ and $h_f/D = 0.75$. In a six-well MTP with $h_f/D = 0.10$ and a 24-well MTP with $h_f/$

D = 0.38, the observed surface-to-volume ratios were rather close, with values of 452 and 435 m^{-1}, respectively and the results of volumetric power input intertwined. Büchs et al. (2001) studied the effect of filling volumes in shaken flasks. Their findings were that for smaller filling volumes in shaken flasks without baffles, the values of volumetric power input increased under the same conditions. This effect can be directly translated to the individual wells, making them display a similar trend and closing the gap between shaken flasks and shaken MTPs. These conditions, however, might lead to other issues such as longer mixing times (Li et al., 2020), which might not be favorable for the operation that is being designed.

3.3 | Correlation of microscale with large scale

The main purpose of this study is to determine how process conditions for downstream unit operations that require mixing and are firstly developed on a microscale can be scaled up to larger systems based on the conservation of volumetric power input. Scale-up of STRs is typically done using the correlations curves of Power number, Ne, to Reynolds number, Re (Nienow, 2014). In our study, the mixing conditions obtained in the MTPs were exemplarily scaled up to laboratory-scale reactors with Rushton impellers. The diameter of the reactors was 60 and 300 mm, respectively. The dimensions and position of the impellers were determined from the standard rules of assembly for stirred tanks (Costes & Couderc, 1988). The calculations of the power input were made for reactors with and without baffles and related to the results from the MTP experiments (Figure 7). Figure 7 shows the conditions of operations that can be obtained in the different MTPs. Minimum and maximum values of volumetric power input obtained in the studied MTPs can be read on the y-axis of the plots. From there, a parallel line to the x-axis was drawn until it reached the plotted curve. From that value of the curve, we drew a parallel to the y-axis up to the x-axis, obtaining the value of the stirring frequency for such power input. The volumetric power input covered by the investigated conditions in the MTPs ranges from about 3 W/m^3 in 6-well plates at 400 rpm on the 3 mm orbital shaker to 250 W/m^3 in 96-well plates at 300 rpm on the 25 mm orbital shaker. The stirring frequencies that can be represented in the microplate experiments are 150–750 rpm for the baffled 60 mm reactor and 200–1100 rpm for the unbaffled reactor of the same inner diameter (Figure 7a). When the diameter of the reactor is increased to 300 mm, MTPs can be used to represent the power input which will be achieved by stirring frequencies within the range of 50–290 rpm in baffled and 60–350 rpm in unbaffled reactors (Figure 7b). Larger vessels require smaller stirring frequencies to maintain constant volumetric power input. The lower stirring frequency can lead to operational problems such as the sinking of particles or longer mixing times than necessary. This creates a limitation in the use of MTPs as a first step for the process design due to the limited coverage of volumetric power input (Hemrajani & Tatterson, 2003). This has been shown and discussed by de Lamotte et al. (2018), who described a 17 L stirred tank system that required 1420 W/m^3 for the motion of

FIGURE 6 Volumetric power input for three different types of wells, 96-, 24-, and 6-well with different filling volumes defined as height-to-diameter ratios on increasing shaking frequencies and on two different shaking diameters, 3 mm (a) and 25 mm (b)
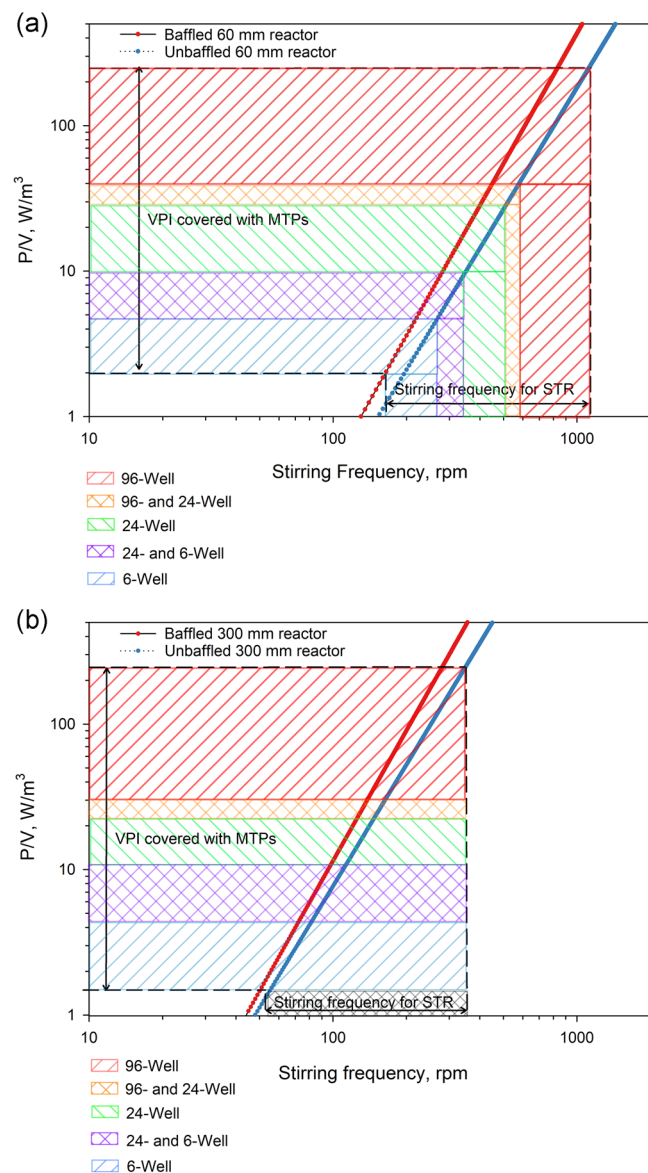
FIGURE 7 Volumetric power input versus stirring frequency for a stirred tank reactor (STR) with a Rushton impeller and covered values of volumetric power input obtained from microplates (MTPs) and applied for two different reactor diameters: 60 mm (a) and 300 mm (b)

water. It is of importance that in contrast to the power input which is indirect proportional to the inner diameter of the well, the shear rate increases with the inner diameter and is the lowest for 96-well plates compared with 24- and 6-well plates. This means that the discussed strategy of constant power input alone would be insufficient for shear-sensitive processes as proven by our research. One system would by far exceed the value of shear rate even though the volumetric power input is the same. An example is the comparison between a 96-well plate at 600 rpm on a 3 mm orbital shaker with and a six-well plate at 175 rpm via a 25 mm orbital shaker, for which a volumetric power input of 31 and 32 W/m³, respectively, was determined. While the power input would be constant, the shear rate is up to 1000 times higher in a well of the 6-well plate compared with a

96-well MTP, as shown in the Supporting Information Material. This would not be an issue for protein solutions (Duerkop et al., 2018) but would be problematic for large bionanoparticles such as viruses and virus-like particles. Therefore, the geometry of MTPs used has to be chosen considering to the shear sensitivity of the systems, also. Another possible issue is the extent to which the degree of turbulence affects the operations when they are taken from MTPs to industrial scales, since the difficulty of their modeling can be complicated.

4 | CONCLUSIONS

From the CFD simulations, we can conclude that the shear rate gradient is highly influenced by the free volume that is contained within the vessel. We also conclude that the filling volume of the wells, which is often not properly described in protocols, is of utmost importance to obtain reliable mixing parameters. The range of power input generated in MTPs reaches from 3 w/m³ in six-well plates to a maximum of 250 W/m³ in 96-well plates with the studied conditions. Within this range of operational conditions, the hydrodynamics of the mixing in the STRs can be simulated in the MTPs which enhances the process development of different downstream operations such as precipitation, flocculation, solubilization, or refolding which depend on mixing. In contrast, the shear stress obtained gets higher the larger the inner diameter of the well is. Therefore, a balance of power input and shear stress determined by the choice of the MTP is important for the design of each individual process step. Considering constant volumetric power input and shear rates depending on the requirements of the unit operation our work allows for a direct scale up of mixing studies from MTPs to STRs in downstream processing.

DATA AVAILABILITY STATEMENT
The data that support the findings of this study are available from the corresponding author upon reasonable request.

ORCID

Alois Jungbauer http://orcid.org/0000-0001-8182-7728
Astrid Dürauer http://orcid.org/0000-0002-6007-7697

REFERENCES

Amanullah, A., Buckland, B. C., & Nienow, A. W. (2003). Mixing in the fermentation and cell culture industries, E. L. Paul, V. A. Atiemo-Obeng & S. M. Kresta, *Handbook of Industrial Mixing* (pp. 1071–1170).John Wiley and Sons.

Azizan, A., Sieben, M., Wandrey, G., & Buchs, J. (2019). Reassessing the out-of-phase phenomenon in shake flasks by evaluating the angle-dependent liquid distribution relative to the direction of the centrifugal acceleration. *Biotechnology and Bioengineering, 116*(11), 2983–2995. https://doi.org/10.1002/bit.27132

Büchs, J., Lotter, S., & Milbradt, C. (2001). Out-of-phase operating conditions, a hitherto unknown phenomenon in shaking bioreactors. *Biochemical Engineering Journal, 7*(2), 135–141. https://doi.org/10.1016/s1369-703x(00)00113-3

Büchs, J., Maier, U., Milbradt, C., & Zoels, B. (2000). Power consumption in shaking flasks on rotary shaking machines: II. Nondimensional description of specific power consumption and flow regimes in unbaffled flasks at elevated liquid viscosity. *Biotechnology and Bioengineering, 68*(6), 594–601. https://doi.org/10.1002/(sici)1097-0290(20000620)68:6%3C594

Costes, J., & Couderc, J. P. (1988). Study by laser Doppler anemometry of the turbulent flow induced by a Rushton turbine in a stirred tank: Influence of the size of the units—I. Mean flow and turbulence. *Chemical Engineering Science, 43*(10), 2751–2764. https://doi.org/10.1016/0009-2509(88)80018-6

de Lamotte, A., Delafosse, A., Calvo, S., & Toye, D. (2018). Identifying dominant spatial and time characteristics of flow dynamics within free-surface baffled stirred-tanks from CFD simulations. *Chemical Engineering Science, 192*, 128–142. https://doi.org/10.1016/j.ces.2018.07.024

Diederich, P., Hoffmann, M., & Hubbuch, J. (2015). High-throughput process development of purification alternatives for the protein avidin. *Biotechnology Progress, 31*(4), 957–973. https://doi.org/10.1002/btpr.2104

Doig, S. D., Pickering, S. C. R., Lye, G. J., & Baganz, F. (2005). Modelling surface aeration rates in shaken microtitre plates using dimensionless groups. *Chemical Engineering Science, 60*(10), 2741–2750. https://doi.org/10.1016/j.ces.2004.12.025

Ducci, A., & Weheliye, W. H. (2014). Orbitally shaken bioreactors-viscosity effects on flow characteristics. *AIChE Journal, 60*(11), 3951–3968. https://doi.org/10.1002/aic.14608

Duerkop, M., Berger, E., Durauer, A., & Jungbauer, A. (2018). Impact of cavitation, high shear stress and air/liquid interfaces on protein aggregation. *Biotechnology Journal, 13*(7), e1800062. https://doi.org/10.1002/biot.201800062

Dürauer, A., Hobiger, S., Walther, C., & Jungbauer, A. (2016). Mixing at the microscale: Power input in shaken microtiter plates. *Biotechnology Journal, 11*(12), 1539–1549. https://doi.org/10.1002/biot.201600027

Effio, C. L., & Hubbuch, J. (2015). Next generation vaccines and vectors: Designing downstream processes for recombinant protein-based virus-like particles. *Biotechnology Journal, 10*(5), 715–727. https://doi.org/10.1002/biot.201400392

Feliciano, J., Berrill, A., Ahnfelt, M., Brekkan, E., Evans, B., Fung, Z., & Łącki, K. (2016). Evaluating high-throughput scale-down chromatography platforms for increased process understanding. *Engineering in Life Sciences, 16*(2), 169–178. https://doi.org/10.1002/elsc.201400241

Hammerschmidt, N., Hobiger, S., & Jungbauer, A. (2016). Continuous polyethylene glycol precipitation of recombinant antibodies: Sequential precipitation and resolubilization. *Process Biochemistry, 51*(2), 325–332. https://doi.org/10.1016/j.procbio.2015.11.032

Hemrajani, R. R., & Tatterson, G. B. (2003). Mechanically stirred vessels, *Handbook of Industrial Mixing* (pp. 345–390).

Hermann, R., Lehmann, M., & Buchs, J. (2003). Characterization of gas-liquid mass transfer phenomena in microtiter plates. *Biotechnology and Bioengineering, 81*(2), 178–186. https://doi.org/10.1002/bit.10456

Hubbuch, J. (2012). Editorial: High-throughput process development. *Biotechnology Journal, 7*(10), 1185–1185. https://doi.org/10.1002/biot.201200333

Li, Y., Ducci, A., & Micheletti, M. (2020). Study on mixing characteristics in shaken microwell systems. *Biochemical Engineering Journal, 153*, 153. https://doi.org/10.1016/j.bej.2019.107392

Micheletti, M., & Lye, G. J. (2006). Microscale bioprocess optimisation. *Current Opinion in Biotechnology, 17*(6), 611–618. https://doi.org/10.1016/j.copbio.2006.10.006

Moreno-González, M., Chuekitkumchorn, P., Silva, M., Groenewoud, R., & Ottens, M. (2021). High throughput process development for the purification of rapeseed proteins napin and cruciferin by ion exchange chromatography. *Food and Bioproducts Processing, 125*, 228–241. https://doi.org/10.1016/j.fbp.2020.11.011

Nienow, A. W. (2014). Stirring and stirred-tank reactors. *Chemie Ingenieur Technik, 86*(12), 2063–2074. https://doi.org/10.1002/cite.201400087

Peter, C. P., Suzuki, Y., Rachinskiy, K., Lotter, S., & Büchs, J. (2006). Volumetric power consumption in baffled shake flasks. *Chemical Engineering Science, 61*(11), 3771–3779. https://doi.org/10.1016/j.ces.2005.12.020

Raval, K., Kato, Y., & Buchs, J. (2007). Comparison of torque method and temperature method for determination of power consumption in disposable shaken bioreactors. *Biochemical Engineering Journal, 34*(3), 224–227. https://doi.org/10.1016/j.bej.2006.12.017

Rodriguez, G., Weheliye, W., Anderlei, T., Micheletti, M., Yianneskis, M., & Ducci, A. (2013). Mixing time and kinetic energy measurements in a shaken cylindrical bioreactor. *Chemical Engineering Research and Design, 91*(11), 2084–2097. https://doi.org/10.1016/j.cherd.2013.03.005

Salek, M. M., Sattari, P., & Martinuzzi, R. J. (2012). Analysis of fluid flow and wall shear stress patterns inside partially filled agitated culture well plates. *Annals of Biomedical Engineering, 40*(3), 707–728. https://doi.org/10.1007/s10439-011-0444-9

Satzer, P., Burgstaller, D., Krepper, W., & Jungbauer, A. (2020). Fractal dimension of antibody-PEG precipitate: Light microscopy for the reconstruction of 3D precipitate structures. *Engineering in Life Sciences, 20*(3-4), 67–78. https://doi.org/10.1002/elsc.201900110

Schulze Wierling, P., Bensch, M., Schroeder, T., & Hubbuch, J. (2005). Automated microscale high-throughput screening for chromatography resins. *Chemie Ingenieur Technik, 77*(8), 1240–1240. https://doi.org/10.1002/cite.200590165

Sieben, M., Giese, H., Grosch, J. H., Kauffmann, K., & Buchs, J. (2016). Permeability of currently available microtiter plate sealing tapes fail to fulfil the requirements for aerobic microbial cultivation. *Biotechnology Journal, 11*(12), 1525–1538. https://doi.org/10.1002/biot.201600054

Somasundaram, B., Pleitt, K., Shave, E., Baker, K., & Lua, L. H. L. (2018). Progression of continuous downstream processing of monoclonal antibodies: Current trends and challenges. *Biotechnology and Bioengineering, 115*(12), 2893–2907. https://doi.org/10.1002/bit.26812

Straathof, A. (2011). The proportion of downstream costs in fermentative production processes. In M. Moo-Young (Eds.) Comprehensive Biotechnology (2nd ed., Volume 2, pp. 811-814), Pergamon, Elsevier.

Tissot, S., Farhat, M., Hacker, D. L., Anderlei, T., Kühner, M., Comninellis, C., & Wurm, F. (2010). Determination of a scale-up

factor from mixing time studies in orbitally shaken bioreactors. *Biochemical Engineering Journal*, *52*(2-3), 181–186. https://doi.org/10.1016/j.bej.2010.08.005

Weheliye, W., Yianneskis, M., & Ducci, A. (2013). On the fluid dynamics of shaken bioreactors- flow characterization and transition. *AIChE Journal*, *59*(1), 334–344. https://doi.org/10.1002/aic.13943

Wutz, J., Steiner, R., Assfalg, K., & Wucherpfennig, T. (2018). Establishment of a CFD-based kL a model in microtiter plates to support CHO cell culture scale-up during clone selection. *Biotechnology Progress*, *34*(5), 1120–1128. https://doi.org/10.1002/btpr.2707

Zhang, H., Lamping, S. R., Pickering, S. C. R., Lye, G. J., & Shamlou, P. A. (2008). Engineering characterisation of a single well from 24-well and 96-well microtitre plates. *Biochemical Engineering Journal*, *40*(1), 138–149. https://doi.org/10.1016/j.bej.2007.12.005

SUPPORTING INFORMATION

Additional supporting information may be found in the online version of the article at the publisher's website.

How to cite this article: Montes-Serrano, I., Satzer, P., Jungbauer, A., & Dürauer, A. (2022). Characterization of hydrodynamics and volumetric power input in microtiter plates for the scale-up of downstream operations. *Biotechnology and Bioengineering*, 119, 523–534. https://doi.org/10.1002/bit.27983